

Role of the Au 5d Orbitals in Bonding: Photoelectron Spectra of [AuMe(PMe<sub>3</sub>)]G. M. BANCROFT,\* T. CHAN, R. J. PUDDPHATT, and J. S. TSE<sup>1</sup>

Received March 4, 1982

The He I and He II photoelectron spectra of [AuMe(PMe<sub>3</sub>)] have been recorded in the gas phase. The spectra have been assigned with use of cross-section arguments, the previously recorded spectra of the analogous molecule Me<sub>2</sub>Hg, and an X $\alpha$  calculation. The two low-binding-energy peaks at 8.24 and 9.22 eV are assigned to the Au-C and Au-P  $\sigma$ -bonding orbitals, respectively. The next three peaks at 9.84, 10.55, and 11.33 eV binding energies are due to the spin-orbit-split Au 5d levels. The d orbital IP's are  $5d_{xy} \approx 5d_{yz} = 10.73$  eV and  $5d_{z^2} = 11.44$  eV. The splitting of 0.71 eV is due to hybridization and bonding of the  $5d_{z^2}$  orbital. The X $\alpha$  calculation and spectral intensities indicate that the Au  $5d_{z^2}$  character is concentrated in the Au-P rather than the Au-C bond. The amount of  $5d_{z^2}$  involvement in bonding is only slightly larger than that of the Hg  $5d_{z^2}$  orbital involvement in Me<sub>2</sub>Hg.

## Introduction

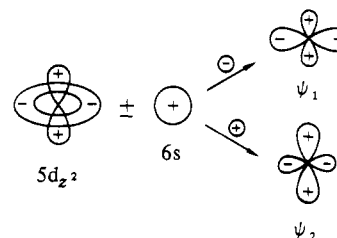
There has been considerable interest in the part played by the filled 5d orbitals of gold in the bonding and reactions of gold(I) compounds. The 5d orbitals are certainly not core orbitals because gold(I) compounds, with linear geometry, often undergo oxidative addition to give square-planar gold(III) complexes with the 5d<sup>8</sup> electron configuration at gold.<sup>2</sup> It has been suggested that electrophilic cleavage of alkyl-gold(I) bonds may occur by initial attack of the electrophile at the metal rather than at the alkyl-gold bond. Since electrophiles will normally attack the highest occupied MO (HOMO), or a filled orbital very close in energy to the HOMO, it is clearly important to know the relative energies of the  $\sigma$ (Au-C) and 5d orbitals in alkylgold(I) complexes, in order to understand these significant reactions.<sup>2,3</sup>

The involvement of 5d orbitals in bonding has been suggested as a chief cause of the high tendency of gold(I) compared to copper(I) or silver(I) to form linear complexes.<sup>4,5</sup> The hypothesis is that mixing of the  $5d_{z^2}$  and 6s orbitals on gold (these orbitals are closer in energy for gold than for copper or silver) gives orbitals  $\psi_1$  and  $\psi_2$  (Scheme I). The electron pair initially in  $d_{z^2}$  can occupy  $\psi_1$ , whose lobes are concentrated in the xy plane away from the ligands, while further hybridization of  $\psi_2$  with  $6p_z$  gives two orbitals with lobes concentrated along the z axis, which then accept electron pairs from the ligands.

Thus although simple crystal field theory would predict that the ordering of d orbitals in linear gold(I) complexes would be  $5d_{z^2}(\sigma) > 5d_{xz}, 5d_{yz}(\pi) > 5d_{xy}, 5d_{x^2-y^2}(\delta)$ ,<sup>5,6</sup> the above effect would lead to a second-order ligand field stabilization of the  $5d_{z^2}$  orbital. This can be illustrated also by a qualitative MO diagram for a  $\sigma$ -bonded complex [AuL<sub>2</sub>]<sup>+</sup>, as shown in Figure 1, the stabilization of  $5d_{z^2}$  arising because the 5d levels are expected to be at lower energy than the  $\sigma$  levels of the ligands.<sup>7</sup>

The degeneracy of  $\pi_g(d_{xz}, d_{yz})$  and  $\delta_g(d_{xy}, d_{x^2-y^2})$  would be split by  $\pi$ -bonding effects in the molecule.

Scheme I



Despite the interest in these molecules, there is very little experimental evidence concerning the d-orbital energies in gold(I) complexes. Mössbauer studies on gold(I) complexes have led to the suggestion that 5d orbitals are not strongly involved in bonding, but the technique would probably not detect minor bonding effects.<sup>8</sup> A study of the electronic spectrum of [Au(CN)<sub>2</sub>]<sup>-</sup> gave the HOMO to be 5d levels with relative energies  $5d_{z^2}(\sigma) > 5d_{xy}, 5d_{x^2-y^2}(\delta) > 5d_{xz}, 5d_{yz}(\pi)$ . This suggests that  $\sigma$  bonding destabilizes  $d_{z^2}$  but  $\pi$  back-bonding stabilizes  $5d_{xz}, 5d_{yz}$  with respect to the  $\delta$ -symmetry orbitals.<sup>9</sup>

Photoelectron spectroscopy has proved to be a powerful method of obtaining molecular orbital information in inorganic and organometallic molecules (for example, see ref 10). However, in many cases such as in a preliminary study of Au and Pt compounds<sup>11</sup> the valence-band spectra are very complex and the assignments very difficult to make with just He I spectra. In this study, we are able to assign the UV photoelectron spectrum of the simple, volatile Au(I) complex [AuMe(PMe<sub>3</sub>)] unambiguously by obtaining high-resolution He I and He II spectra, by comparison of the spectrum with that of Me<sub>2</sub>Hg<sup>6,12,13</sup> and with the aid of X $\alpha$  calculations on the model compound [AuMe(PH<sub>3</sub>)]. Somewhat surprisingly, all our evidence indicates that the involvement of the Au  $5d_{z^2}$  orbitals in bonding is only slightly greater than that of the Hg  $5d_{z^2}$  orbital in Me<sub>2</sub>Hg.

## Experimental Section

(a) **Photoelectron Spectra.** [AuMe(PMe<sub>3</sub>)] was prepared according to literature methods.<sup>14</sup> The white crystals had a melting point of 74-75 °C. The proton NMR spectrum in Me<sub>2</sub>Si showed two doublets of intensity ratio 3:1 having  $\delta$ 's of 1.4 and 0.3 and coupling constants of 10 Hz due to the PMe<sub>3</sub> and Me protons, respectively. The He I

(1) Present address: Colloid and Clathrate Chemistry, National Research Council, Ottawa, Canada.

(2) (a) J. K. Kochi, "Organometallic Mechanisms and Catalysis", Academic Press, New York, 1978, pp 534, 566; (b) A. Tamaki and J. K. Kochi, *J. Chem. Soc., Dalton Trans.*, 2620 (1973).

(3) D. A. Slack and M. C. Baird, *J. Am. Chem. Soc.*, **98**, 5539 (1976).

(4) L. E. Orgel, *J. Chem. Soc.*, 4186 (1958); C. K. Jørgensen and J. Pouradier, *J. Chim. Phys. Phys.-Chim. Biol.*, **67**, 124 (1970).

(5) The theory is discussed frequently in modern textbooks: F. A. Cotton and G. Wilkinson, "Advanced Inorganic Chemistry", 4th ed., Wiley, New York, 1980, p 969; J. E. Huheey, "Inorganic Chemistry", 2nd ed., Harper and Row, New York, 1978, p 427.

(6) (a) P. Burroughs, S. Evans, A. Hamnett, A. F. Orchard, and N. V. Richardson, *J. Chem. Soc., Chem. Commun.*, 921 (1974); (b) D. K. Creber and G. M. Bancroft, *Inorg. Chem.*, **19**, 643 (1980), and references therein.

(7) This ordering with  $\sigma$  levels higher in energy than d-block levels is fully consistent with extended Hückel calculations on molecules MeAu and Me<sub>2</sub>Au by Hoffmann and co-workers: S. Komiyama, T. A. Albright, R. Hoffmann, and J. K. Kochi, *J. Am. Chem. Soc.*, **98**, 7255 (1976); **99**, 8440 (1977).

(8) P. G. Jones, A. G. Maddock, M. J. Mays, M. M. Muir, and A. F. Williams, *J. Chem. Soc., Dalton Trans.*, 1434 (1977).

(9) W. R. Mason, *J. Am. Chem. Soc.*, **98**, 5182 (1976).

(10) A. H. Cowley, *Prog. Inorg. Chem.*, **26**, 45 (1979).

(11) J. Behan, R. A. W. Johnstone, and R. J. Puddephatt, *J. Chem. Soc., Chem. Commun.*, 444, (1978).

(12) T. P. Fehlner, J. Ulman, W. A. Nugent, and J. K. Kochi, *Inorg. Chem.*, **15**, 2544 (1976).

(13) L. L. Coatsworth, G. M. Bancroft, D. K. Creber, R. J. D. Lazier, and P. W. M. Jacobs, *J. Electron Spectrosc. Relat. Phenom.*, **13**, 395 (1978).

(14) H. Schmidbaur and A. Shiotani, *Chem. Ber.*, **104**, 2821 (1971).

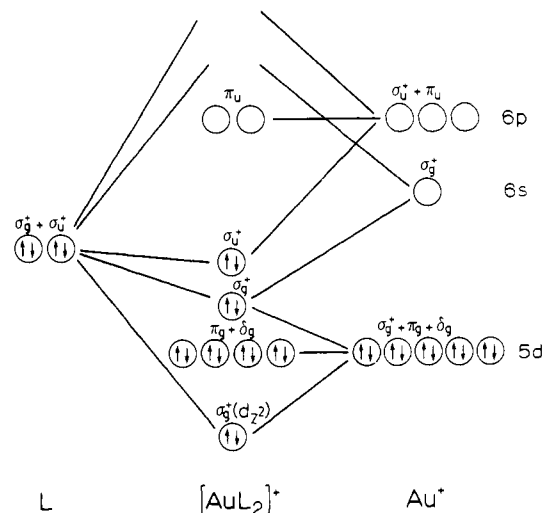


Figure 1. Qualitative MO diagram for a  $\sigma$ -bonded complex  $[\text{AuL}_2]^+$ .

and He II spectra were recorded in the gas phase with a McPherson ESCA 36 spectrometer using a hollow-cathode lamp<sup>13</sup> and our high-temperature solid-state insert.<sup>15</sup> Spectra were obtained at a cell temperature of  $\sim 65^\circ\text{C}$  and calibrated with the Ar  $3p_{3/2}$  line at 15.759 eV.

The Ar  $3p_{3/2}$  line widths before the compound was run were 17 and 27 meV with He I and He II radiation, respectively. After spectra were run for several hours, the Ar 3p line width never was greater than 40 meV. All spectra were fitted to Lorentzian-Gaussian line shapes with use of an iterative procedure described earlier.<sup>16</sup>

(b) SCF-X $\alpha$ -SW Calculations. As an aid for the spectral assignments, an SCF-X $\alpha$ -SW calculation was performed on the model compound  $[\text{AuMe}(\text{PH}_3)]$ . Coordinates for  $[\text{AuMe}(\text{PH}_3)]$  in atomic units were derived from the experimental bond parameters  $r(\text{P-H}) = 1.415 \text{ \AA}$ ,<sup>17</sup>  $\angle\text{H-P-H} = 93.45^\circ$ ,<sup>18</sup>  $r(\text{Au-P}) = 2.279 \text{ \AA}$ ,<sup>19</sup>  $r(\text{Au-C}) = 2.124 \text{ \AA}$ ,<sup>19</sup>  $r(\text{C-H}) = 1.01 \text{ \AA}$ , and  $\angle\text{H-C-H} = 109.5^\circ$ , with the assumption that  $[\text{AuMe}(\text{PH}_3)]$  has  $C_{3v}$  symmetry.

The  $\alpha_{\text{HF}}$  exchange parameters for P, H, Au, and C were taken from the tabulation of Schwarz.<sup>20</sup> For the extramolecular and intersphere regions, a weighted-average  $\alpha$  was used where the weights were the number of valence electrons (11 for Au, 5 for P, 4 for C, 1 for H). This seems to be a sensible choice since only the valence electrons have significant probability density outside the atomic spheres.

Norman's "nonempirical" method<sup>21</sup> was used to obtain the ratio of atomic sphere radii. The initial X $\alpha$ -SW molecular charge distribution was examined to determine the radii  $R_i$  of each atomic sphere  $i$  which just enclose the number of electrons put in for the atom when the free-atom charge density was calculated. The ratios of atomic spheres for the SCF calculation are taken equal to the ratios of the  $R_i$ 's. Overlapping sphere radii (10%) were used as an approximation for the non-muffin-tin corrections. The basic idea is to pick up extra-large amounts of charge near the atomic spheres that extend into the interatomic regions. The outer-sphere radius was chosen such that it is just touching all H's. Outer-sphere coordinates were centered at the weighted-average position of all the atoms and were calculated with use of the same method as that for  $\alpha_{\text{out}}$ . Coordinates,  $\alpha$  parameters, and sphere radii are summarized in Table I.

$C_{3v}$  full symmetry was employed to factor the secular matrix. The molecular wave functions were expanded with  $l = 4$  in the extramolecular region,  $l = 3$  in the Au region,  $l = 2$  in the carbon and phosphorus region, and  $l = 1$  in the hydrogen regions. Core levels were frozen initially and later released in the SCF calculation. The convergence criterion was  $\epsilon \leq 10^{-3}$  Ry. It is noteworthy that the

Table I. Parameters Used in Overlapping-Spheres (10%) X $\alpha$ -SW Calculations for  $\text{AuMe}(\text{PH}_3)$

region	x	y	z	$\alpha$	sphere radii
Au	0	0	0	0.6930	2.541
P	0	0	-4.3067	0.7262	2.196
C	0	0	4.0138	0.75928	1.726
H <sub>1</sub> (C)	1.9620	0	0	0.77725	1.240
H <sub>2</sub> (C)	-0.9810	1.6991	4.7063	0.77725	1.240
H <sub>3</sub> (C)	-0.9810	-1.6991	4.7063	0.77725	1.240
H <sub>4</sub> (P)	2.7480	0	-5.7547	0.77725	1.357
H <sub>5</sub> (P)	-1.1240	1.9469	-5.7547	0.77725	1.357
H <sub>6</sub> (P)	-1.1240	-1.9469	-5.7547	0.77725	1.357
extramolecular	0	0	-0.2815	0.7290	7.6159

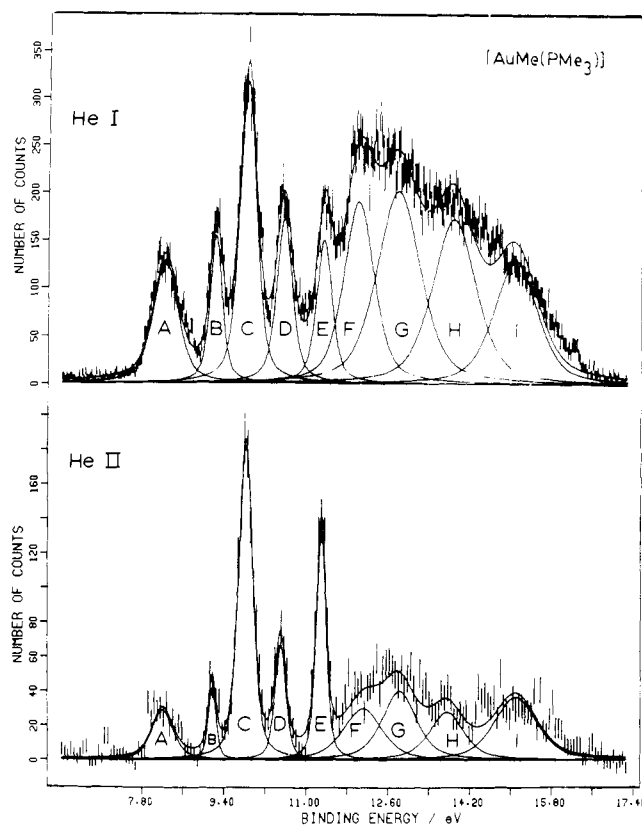


Figure 2. He I and He II photoelectron spectra of  $[\text{AuMe}(\text{PMe}_3)]$ . The spectra are calibrated relative to the Ar  $3p_{3/2}$  level at 15.759 eV.

numerical values of the ground-state X $\alpha$ -SW eigenvalues cannot be compared directly with those from Hartree-Fock calculations since the one-electron eigenvalue concept is different for the two methods.<sup>22</sup> Generally, the eigenvalues obtained with use of the transition-state potential of the HOMO (by removal of half an electron) are compared with the experimental values.

## Results and Discussion

(a) SCF-X $\alpha$ -SW Calculation. The calculated total energy for  $[\text{AuMe}(\text{PH}_3)]$  is  $-3650.12$  Ry, and the virial ratio is 1.0002. The final intersphere potential is  $-0.3367$  Ry. The ionization potentials for the molecular orbitals were calculated with use of Slater's transition-state method with half of an electron removed from the HOMO  $\sigma(\text{Au-C})$ . The ionization or binding energies and the ground-state charge distributions from these calculations are listed in Table II. Several important trends are apparent in Table II. First, the Au-C orbital has a smaller IP than the Au-P orbital. Second, all the Au 5d levels have IP's larger than those of the two bonding orbitals above and the orbital energy ordering is  $d_\pi > d_\delta >$

- (15) G. M. Bancroft, D. J. Bristow, and L. L. Coatsworth, *Chem. Phys. Lett.*, **82**, 344 (1981).  
 (16) G. M. Bancroft, I. Adams, L. L. Coatsworth, C. D. Bennowitz, J. D. Brown, and W. D. Westwood, *Anal. Chem.*, **47**, 536 (1975).  
 (17) K. Kuchitzer, *J. Mol. Spectrosc.*, **7**, 399 (1961).  
 (18) M. H. Sivertz and R. E. Weston, Jr., *J. Chem. Phys.*, **21**, 898 (1953).  
 (19) P. D. Gavens, J. J. Guy, M. J. Mays, and G. M. Sheldrick, *Acta Crystallogr., Sect. B*, **B33**, 137 (1977).  
 (20) K. Schwarz, *Phys. Rev. B: Solid State*, **5**, 2466 (1972).  
 (21) J. G. Norman, Jr., *J. Chem. Phys.*, **61**, 4630 (1974).

- (22) J. C. Slater and K. H. Johnson, *Phys. Rev. B: Solid State*, **5**, 844 (1972).

Table II. Valence-Level Energies and Charge Distributions for AuMe(PH<sub>3</sub>)

level	energy, <sup>b</sup> eV	% charge distribn <sup>a</sup>						
		Au	P	C	H <sub>p</sub>	H <sub>c</sub>	inter	outer
Au-C	7.25	25.30 (s)	1.70	30.55 (p)	3.3	0.22	37.69	1.23
Au-P	9.58	34.64 (d)	31.02 (p)	3.96	0.54	6.75	22.12	0.96
5d <sub>π</sub>	11.77	52.00 (d)	1.05	18.29	21.84	1.65	4.84	0.32
5d <sub>σ</sub>	12.31	92.64 (d)	0.07	0.02	0.00	0.09	7.18	0.00
C-H(Au)	12.90	34.82 (d)	1.96 (p)	25.04	25.62	3.18	9.10	0.30
P-H	13.43	5.52 (p)	38.24	0.34	0.30	45.06	9.64	0.91
5d <sub>σ</sub>	14.0	61.35 (d)	20.87 (p)	4.52	2.04	5.70	5.11	0.36
C-H	19.25	3.15	0.55	54.77 (s)	34.02	0.36	6.88	0.29
P-H	20.03	2.43	61.88 (s)	0.33	0.15	27.75	6.97	0.50

<sup>a</sup> The characters of the predominant atomic orbitals are in parentheses. <sup>b</sup> Calculated with the transition potential of HOMO (Au-C).

Table III. Photoelectron Parameters for the He I and He II Spectra of [AuMe(PMe<sub>3</sub>)]

peak	level	binding energy, <sup>a</sup> eV	fwhm, eV	area <sup>b</sup>	
				He I	He II
A	Au-C	8.24	0.56	0.6	0.4
B	Au-P	9.22	0.28	0.5	0.3
C	Au d <sub>3/2</sub>	9.84	0.38	1.0	1.72
D	Au d <sub>σ</sub>	10.55	0.36	0.8	0.6
E	Au d <sub>3/2</sub>	11.33	0.30	0.6	1.0
F	P-C	12.00	0.7	1.7	0.5
G, H, I	C-H	12.7-15.0	1.0	7.8	3.4

<sup>a</sup> The He I and He II binding energies agree to within 0.04 eV.

<sup>b</sup> Experimental intensities are divided by the peak kinetic energy and normalized to the Hg 5d<sub>5/2</sub> cross section<sup>24</sup> (see text).

d<sub>σ</sub>, as was found previously for Me<sub>2</sub>Hg.<sup>13</sup> This ordering implies that there is some involvement of d<sub>σ</sub> in σ bonding, to the methyl and phosphine ligands. Third, the charge distributions indicate that the Au-P orbital has substantial Au 5d character, while the Au-C orbital has no significant Au 5d character.

**(b) Assignment of the He I and He II Photoelectron Spectra.** The He I and He II photoelectron spectra of [AuMe(PMe<sub>3</sub>)] are shown in Figure 2, and the peak positions, widths, relative intensities, and assignments are given in Table III. Five distinct peaks (A-E) are obvious in the low-binding-energy region in both the He I and the He II spectra. Peak F is reasonably well-defined in the He I spectrum, but the peaks at higher binding energy (G-I) have been fitted only to simulate both spectra in a consistent manner and to obtain approximate areas under the broad envelopes.

Peaks C, D, and E can be assigned immediately to Au 5d orbitals from the marked intensity changes between the He I and He II spectra, combined with the previously published spectra of the analogous Me<sub>2</sub>Hg molecule.<sup>7</sup> In Me<sub>2</sub>Hg, the three Hg 5d peaks in the broad-scan spectra at 15.0, 15.4, and 16.9 eV<sup>6</sup> are well separated from the rest of the valence-band region, and the separation between the outer two peaks of 1.9 eV is just the atomic Hg 5d spin-orbit splitting.<sup>23</sup> All three Hg 5d peaks increase in intensity relative to the valence-band peaks on going from He I to He II spectra, although the middle peak of 15.4 eV decreases substantially relative to the other two Hg 5d peaks. Such increases in metal d cross sections from He I to He II spectra are well-known.<sup>7,23</sup> Peaks C, D, and E in the [AuMe(PMe<sub>3</sub>)] spectra show a photon energy dependence very similar to that of the three Hg 5d peaks, and the separation of the outer two peaks C and E (1.49 eV) is very similar to the atomic Au spin-orbit splitting of 1.52 eV.<sup>24</sup> As for Me<sub>2</sub>Hg, the middle peak D decreases relative to the other two d peaks on going from the He I to He II spectra. A more detailed discussion of these d peaks follows in the next section.

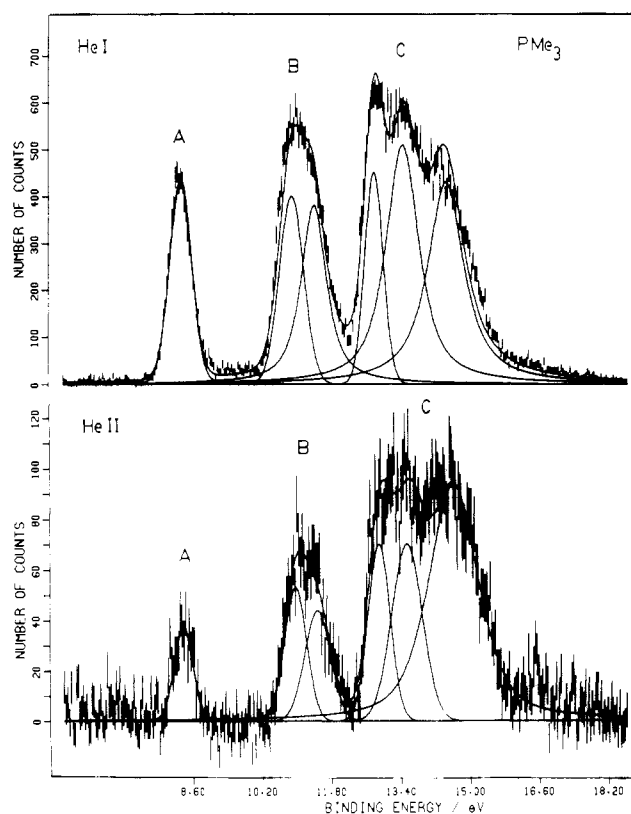


Figure 3. He I and He II photoelectron spectra of PMe<sub>3</sub>. The spectra are calibrated relative to the Ar 3p<sub>3/2</sub> level at 15.759 eV.

Table IV. Binding Energies for the PMe<sub>3</sub> Photoelectron Spectra (eV)

orbital	exptl energy		widths this work
	this work	ref 25	
8a <sub>1</sub>	8.62	8.58	0.59
6e	11.13, 11.70	11.31	0.66, 0.70
1a <sub>2</sub>	13.02-14.68	12.7-15.8	
5e			
7a <sub>1</sub>			
4e			

The two low-binding-energy peaks at 8.24 and 9.22 eV can be assigned readily to the Au-C and Au-P σ-bonding orbitals, respectively. This assignment is supported by the X<sub>α</sub> calculations (Table II). The photoelectron spectra of PMe<sub>3</sub> (Figure 3, Table IV) also support this assignment. The low-binding-energy peak at 8.62 eV arises from the 8a<sub>1</sub> P lone-pair orbital.<sup>25</sup> Due to bonding to Au, one would expect the Au-P IP to be larger than this value, thus pointing to peak B at 9.22 eV as

(23) S. Suzer, P. R. Hilton, N. S. Hush, and S. Nordholm, *J. Electron Spectrosc. Relat. Phenom.*, **12**, 357 (1977).

(24) C. E. Moore, *Natl. Bur. Stand. (U.S.), Circ.*, No. 467 (1958).

(25) I. H. Hillier and U. R. Saunders, *J. Chem. Soc., Faraday Trans.*, 2401 (1970).

Table V. Comparison of the Metal 5d Photoelectron Spectra of  $\text{Me}_2\text{Hg}$  and  $[\text{AuMe}(\text{PMe}_3)]$ 

approx term	binding energy, eV		approx term	binding energy, eV	
	$\text{Me}_2\text{Hg}$	$[\text{AuMe}(\text{PMe}_3)]$		$\text{Me}_2\text{Hg}$	$[\text{AuMe}(\text{PMe}_3)]$
$\Pi_{3/2}$	14.91	} 9.84	$\Pi_{1/2}$	} 16.9	} 11.33
$\Delta_{5/2}$	14.95		$\Delta_{3/2}$		
$\Sigma_{1/2}$	15.4	10.55			

arising from the Au-P orbital. This change in the P lone-pair IP on bonding is similar to that found for  $\text{PF}_3$ .<sup>26</sup> The IP for the phosphorus lone-pair orbital in  $\text{PF}_3$  is found to be at 12.3 eV. Upon complex formation in  $[\text{Pt}(\text{PF}_3)_4]$ , the Pt-P IP is increased to 14.5 eV.

The width of peak A (0.56 eV) is about twice that of B (0.28 eV), and these relative widths are consistent with our assignment. The large Au-C width is similar to the large M-C ( $\text{M} = \text{Zn}, \text{Cd}, \text{Hg}$ ) widths ( $\geq 0.5$  eV) obtained for other  $\text{Me}_2\text{M}$  compounds.

Peaks F-I can now be assigned with the aid of the  $\text{PMe}_3$  spectra. Peak F at 12.00 eV has a larger IP than the average of the two P-C peaks at 11.23 eV due to donation of electrons from the phosphine to the metal. Peaks G-I between 12.7 and 15.0 eV are just in the range of both C-H  $\sigma$ -bonding orbitals in  $\text{CH}_3$  in other metal alkyls<sup>7</sup> and  $\text{PMe}_3$  (Table IV).

(c) **Au 5d<sub>σ</sub> Participation in Bonding.** We now assign the Au d orbitals and cross-section variations in more detail to extract more subtle bonding information. As for the Hg 5d orbitals in  $\text{Me}_2\text{Hg}$ ,<sup>6,7,13</sup> the Au 5d orbitals in  $[\text{AuMe}(\text{PMe}_3)]$  can be split by the combination of crystal (or ligand) field splitting and bonding outlined in the Introduction, coupled with spin-orbit splitting in the 5d<sup>9</sup> ion state. This <sup>2</sup>D final state is split by spin-orbit splitting into <sup>2</sup>D<sub>5/2</sub> and <sup>2</sup>D<sub>3/2</sub> states, which can be split further into  $\Delta_{5/2}$ ,  $\Pi_{3/2}$ ,  $\Sigma_{1/2}$  and  $\Delta_{3/2}$ ,  $\Pi_{1/2}$  due to the combined effects of crystal field splitting and bonding.<sup>27</sup> With just spin-orbit and crystal field splitting (as for the Cd 4d levels in  $\text{Me}_2\text{Cd}$ ),<sup>28</sup> the order of multiplet states is  ${}^2\Delta_{3/2} > {}^2\Pi_{1/2} > {}^2\Delta_{5/2} > {}^2\Pi_{3/2} > \Sigma_{1/2}$ , where the first two of these states are derived mostly from <sup>2</sup>D<sub>3/2</sub> and the latter three mostly from <sup>2</sup>D<sub>5/2</sub>. This order corresponds to the crystal field orbital order  $d_\pi > d_x > d_z$  mentioned in the Introduction. However, for  $\text{Me}_2\text{Hg}$  and  $[\text{AuMe}(\text{PMe}_3)]$ , the splitting due to bonding of  $d_\sigma$  is far larger than crystal field splitting, and the  $\Sigma_{1/2}$  peak moves out of the D<sub>5/2</sub> envelope to higher binding energy. As for  $\text{Me}_2\text{Hg}$ , then, the order of states becomes  ${}^2\Delta_{3/2} \approx {}^2\Pi_{1/2}$  (peak E)  $> {}^2\Sigma_{1/2}$  (peak D)  $> {}^2\Delta_{5/2} \approx {}^2\Pi_{3/2}$  (peak C) (Table V), which corresponds to the orbital energy ordering  $d_\pi \approx d_\delta > d_\sigma$ . In  $\text{Me}_2\text{Hg}$ , we were able to resolve all five peaks,<sup>13</sup> due to the very narrow widths of  $\leq 0.04$  eV. However, in  $[\text{AuMe}(\text{PMe}_3)]$ , the very much broader peaks preclude resolving peaks C and E into component peaks.

In both  $\text{Me}_2\text{Hg}$  and  $\text{AuMe}(\text{PMe}_3)$ , the involvement of the metal 5d<sub>σ</sub> electrons in bonding does not appear to be very large. To first order, the 5d<sub>σ</sub> orbital is stabilized by 0.71 eV (10.55 - 9.84) in the Au compound—slightly larger than the 0.45-eV stabilization in  $\text{Me}_2\text{Hg}$ . After the spin-orbit splitting is subtracted out, the orbital energies for the Au compound are

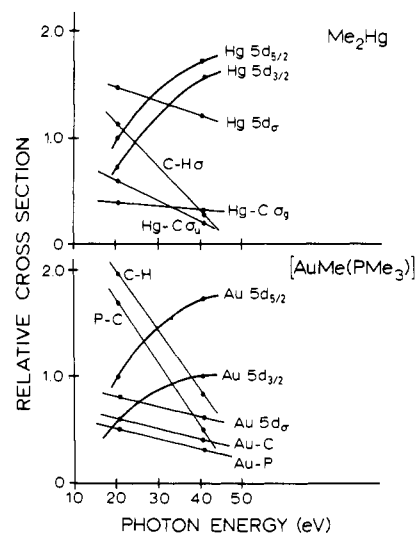


Figure 4. Plots of relative cross sections for  $\text{Me}_2\text{Hg}$ <sup>6</sup> and  $[\text{AuMe}(\text{PMe}_3)]$ .

$d_\pi$ ,  $d_x = 10.44$  eV and  $d_\sigma = 11.15$  eV. The X $\alpha$  calculation overestimates the splitting of the d orbitals greatly (Table II) but does give the correct ordering.

The cross sections shown in Figure 4 further confirm our assignments and also show the involvement of the Au 5d<sub>σ</sub> orbital in bonding. For the  $[\text{AuMe}(\text{PMe}_3)]$  plot in Figure 4b we assume that the Au d cross sections are the same as those for neighboring atomic Hg.<sup>23</sup> Recent cross-section tables<sup>29</sup> indicate that this is a reasonable assumption. We then normalize all cross sections to these atomic values. The metal  $d_{5/2}$  and  $d_{3/2}$  cross sections rise rapidly on going from He I to He II photon energies. In the Au compound, the Au-C and Au-P cross sections decrease a small amount, but this parallel trend is still consistent with the high Au 5d character in the Au-P bond from the X $\alpha$  calculation (Table II). From the  $\text{PMe}_3$  spectra (Figure 3), we would expect the P lone-pair intensity to decrease dramatically from He I to the He II spectrum of  $[\text{AuMe}(\text{PMe}_3)]$  relative to those of the P-C and C-H peaks, but instead it is relatively more intense than these peaks. This strongly indicates that there is substantial Au d character in the Au-P molecular orbital. The Au-C cross section changes in a manner similar to that for M-C orbitals in  $\text{Me}_2\text{M}$  ( $\text{M} = \text{Zn}, \text{Cd}$ ) compounds and the Hg-C  $\sigma_u$  orbital<sup>6</sup> in  $\text{Me}_2\text{Hg}$  in which there is no d-orbital involvement. This, then, is also consistent with the X $\alpha$  calculation, which shows no Au 5d character in the Au-C orbital.

The apparent small difference between Hg 5d<sub>σ</sub> and Au 5d<sub>σ</sub> involvement in bonding is perhaps surprising considering first that the Au 5d orbitals are within 1 eV of the Au-P orbital, while the Hg 5d orbitals are  $> 3$  eV from the Hg  $\sigma_g$  orbital, and second that the 5d<sup>9</sup>6s state in  $\text{Au}^+$  is 1.86 eV above the ground state, while that for the 5d<sup>9</sup>6s state in  $\text{Hg}^{2+}$  is 5.31 eV above the ground state.<sup>4</sup> Rather small energy differences for the d<sup>9</sup>s states in  $\text{Cu}^+$  (2.72 eV) and  $\text{Au}^+$  are often used to rationalize the greater tendency of Au to form linear complexes.

**Acknowledgment.** We are very grateful to the Natural Sciences and Engineering Research Council of Canada (NSERC) for financial support and D. J. Bristow and E. Pellach for technical assistance.

Registry No.  $\text{AuMe}(\text{PMe}_3)$ , 32407-79-7.

(26) I. H. Hillier, *Pure Appl. Chem.*, **51**, 2183 (1979).

(27) The use of term symbols here is meant only to assign majority character to these levels. From previous studies,<sup>28</sup> the  $\Delta_{5/2}$  is of pure  $d_x$  character ( $m_l = \pm 2$ ), whereas the other levels are only "majority"  $\Delta$ ,  $\Pi$ , and  $\Sigma$  character.

(28) G. M. Bancroft, D. K. Creber, and H. Basch, *J. Chem. Phys.*, **67**, 4891 (1977).